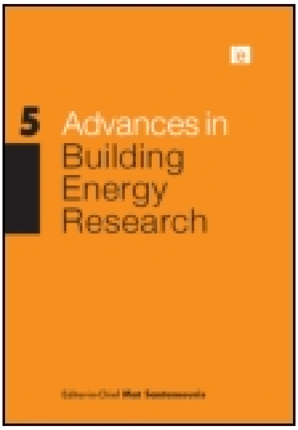

Advances in Building Energy Research
Publication details, including instructions for authors and subscription information:
http://www.tandfonline.com/loi/taer20

The climate effects of increasing the albedo of roofs in a cold region†

Ali Gholizadeh Touchaei[a] & Hashem Akbari[a]
[a] Building, Civil and Environmental Engineering Department, Concordia University, 1455, de Maisonneuve Blvd. West, EV006.409, Montreal, Quebec, Canada H3G 1M8
Published online: 20 Dec 2013.

Advances in Building Energy Research, 2013
Vol. 7, No. 2, 186–191, http://dx.doi.org/10.1080/17512549.2013.865558

Taylor & Francis
Taylor & Francis Group

The climate effects of increasing the albedo of roofs in a cold region†

Ali Gholizadeh Touchaei and Hashem Akbari*

Building, Civil and Environmental Engineering Department, Concordia University, 1455, de Maisonneuve Blvd. West, EV006.409, Montreal, Quebec, Canada H3G 1M8

Urban heat island (UHI) phenomenon has been observed in many large cities located in cold regions (e.g. Montreal in Canada) during summer. One of the well-known strategies to mitigate the temperature rise of urban areas is increasing their albedo. Roofs cover about 25% of urban areas and increasing their reflectivity would have a significant effect on the total energy budget of a city. We have studied the effect of increasing the albedo of roofs on the air and skin temperature distributions of the Greater Montreal area. We performed simulations for one-day summer episode (12 July 2005) using the Weather Research and Forecasting (WRF) mesoscale model. The WRF solver (version 3.4.1) is coupled with three different urban canopy models (UCMs): slab, single-layer, and multi-layer. We used all three UCMs by increasing the roof albedo from 0.2 to 0.8 and compared the results. All models simulated a well-defined UHI over areas with high concentration of roofs. They predicted a maximum air temperature decrease of about 1 K by implementing cool roofs. The difference between the skin (surface) temperature of urban area and its surrounding was about 9 K. The maximum air temperature difference between the urban and suburban areas was about 4 K.

Keywords: urban heat island; urban canopy model; Albedo; mitigation strategies; WRF

1. Introduction

Urban areas are usually warmer than their surroundings; this phenomenon is called urban heat island (UHI) (Keefer, 2012). Figure 1 illustrates the typical surface temperature variation along a city, maximum temperature occurs in its urban area. UHI can increase the average air temperature of an urban area 1–3 K more than its surrounding (EPA, 2012). UHI have considerable nocturnal effect (Figure 2) and the temperature difference can be as high as 12 K (Oke, 1987; Roth, Oke, & Emery, 1989). UHI affects a large vertical region above cities, for instance, Bornstein (1968) reported the temperature difference between New York City and its surrounding have been extended over 500 m in mornings.

Two main strategies to mitigate UHI are: (1) cool surfaces and (2) vegetating surfaces (including roofs). The focus of this paper is on studying the effect of cool surfaces on urban climate.

Cool materials have both high solar reflectance and high thermal emittance (Levinson, Akbari, & Berdahl, 2005). Using cool materials for roofs and pavements decreases the heat absorption of urban surfaces. The reflectivity of urban surfaces is known as “Albedo” and increasing the albedo can reduce the temperature of the urban areas and consequently the UHI intensity.

†Earlier version of this paper is presented in the 34th AIVC conference, Athens, Greece, 25–26 September 2013.

*Coresponding author. Email: hashem.akbari@concordia.ca

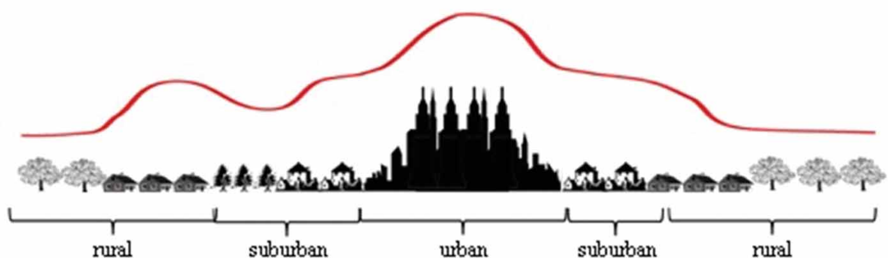

Figure 1. Typical variation of surface temperature along a city and occurrence of the UHI.

Here, the effect of increasing roofs reflectivity in Montreal is simulated by using three standard urban canopy models (UCM) of the Weather Research and Forecasting model (WRF). Multilayer UCM (ML-UCM) is more accurate than other types of UCM because it can consider the effect of turbulence. However, other two types of UCM (slab and single layer) are much faster in computation time. Applicability of slab model and single-layer UCM (SL-UCM) for urban climate modeling is compared with ML-UCM. All UCMs were coupled with WRF to simulate a single day in summer and characterize UHI at 2 m height. The skin temperature distribution was also quantified.

2. Simulation

WRF version 3.4.1 was used for the simulation of the urban climate. For Greater Montreal, the simulation domain was 100 × 100 km centered at ~45.5°N and ~73.6°W (Figure 3 shows the areas of interest cropped from the original domain). Size of the grids was in the order of a neighborhood (333 × 333 m). Figure 3 shows the satellite image of the selected city (on left) and its land-use categories (on right). Land use was standard 24-category U.S. Geological Survey (USGS) implemented within WRF. Urban areas of the city are illustrated in Figure 3 in black. Simulation periods started from 11 July 2005 1200 UTC (11 July 2005 0800 LST) to 13 July 2005 1200 UTC (13 July 2005 0800 LST). First 16 h is considered as spin-up time and outputs of next 24 h of simulations analyzed (12 July LST). Initial and boundary conditions of

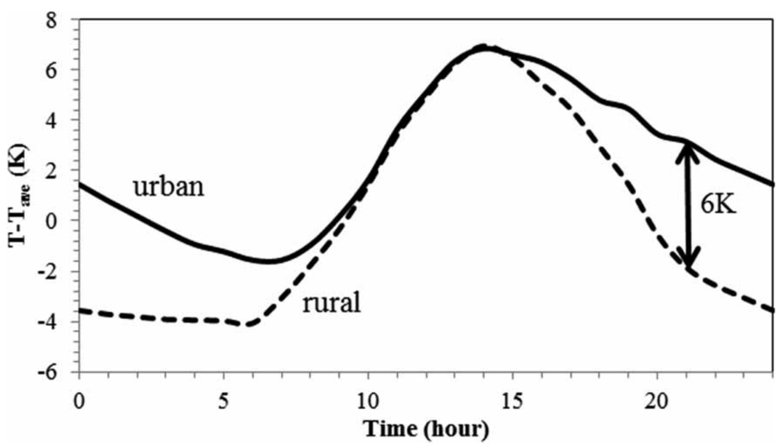

Figure 2. Typical temporal variation of urban and rural surface temperature from its daily average.

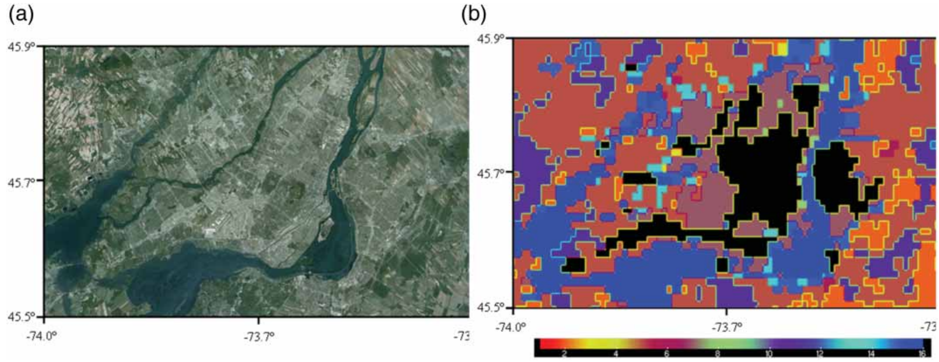

Figure 3. (a) Simulation domain (http://maps.google.ca) and (b) land-use land cover of Greater Montreal extracted from USGS dataset (Black regions are urban areas).

the simulations extracted from 3-h, high resolution 32 km, North America Regional Reanalysis data (Mesinger et al., 2006).

Planetary boundary layer (PBL) accounts for the exchange of vertical heat and momentum from the ground on the whole air column of the grid cell. The surface-layer model provides interaction between lower level (from land-surface model) and PBL. A land-surface model (LSM) provides information of heat and moisture fluxes on land points and sea ice using atmospheric feedback of other schemes in a simulation (it can be considered as a boundary condition for PBL). LSM updates surface variables (e.g. the ground temperature, soil temperature profile, soil moisture profile, snow cover, and canopy properties) in each iteration step as independent variables. PBL is simulated by the Mellor-Yamada-Janjic scheme (Janjic, 1990, 1994) using Eta similarity theory (surface-layer scheme) (Janjic, 2002). The only available option in WRF for land-surface scheme is Noah-LSM (Chen & Dudhia, 2001). Microphysics models calculate the process of transforming water from one form (rain, snow, graupel, vapor, etc.) to another form. In general, water vapor creates cloud water and cloud ice to shape snow, rain, and other types of precipitation. The Lin scheme (Lin, Farley, & Orville, 1983) was used, as the microphysics option comprises six classes of hydrometeors. The Cumulus model estimates the effect of cloud convection in a grid. The Grell 3D option based on the Grell-Devenyi ensemble scheme (Grell & Devenyi, 2002) was used for cumulus parameterization. Radiation models determine different radiation processes in the atmosphere (incoming shortwave from the sky, longwave radiation from clouds, absorption by aerosols in the atmosphere, etc.). A new rapid radiative transfer model (named "RRTMG") was selected to simulate the longwave radiation (Clough et al., 2005). The Goddard scheme was employed to estimate the shortwave radiation by considering the effect of ozone and cloud (Chou & Suarez, 1994).

Simulations were performed without applying any damping option (a method to increase the stability of the mesoscale model by reducing the vertical velocity) according to the short period of running. Positive definite advection options for turbulent kinetic energy, moisture, and scalars were activated. Monthly background albedo is the standard input of the software and it is based on measurements of the advanced very high resolution radiometer. In the slab model, albedo of the urban areas is considered to be 0.15 (this value is corrected from 0.18 by Liu, Chen, Warner, and Basara (2006) to account for radiation trapping in the canopy). In single and ML-UCMs, albedo of urban areas is estimated based on albedo of urban surfaces (i.e. roof, wall, and road). By default, all urban surfaces are considered to be 20% reflective. However, the effective albedo of the urban area changes during a day by the position of sun.

3. Results and discussions

Results are divided into three parts: (1) evaluation of UCMs, (2) observation of UHI in Montreal, and (3) effect of increasing surface albedo on urban temperature.

3.1. *Evaluation of UCMs*

Simulation of a case with ML-UCM increases the computation time by 30–40% with respect to the time needed for the slab model and SL-UCM. Figure 4 shows the average air and skin temperatures difference between ML-UCM with other two models. Based on these simulations, temperature difference of up to 1 K is observed. Although SL-UCM and the slab model in WRF were tested for mesoscale modeling, for fine resolution and the scale of urban they are not appropriate. Hence, we used ML-UCM in the rest of the study. Our simulations for other cities than Montreal produced similar results.

3.2. *Observation of UHI in Montreal*

To find the difference between the air and skin temperatures of urban and rural areas, some random points in each region were selected. We considered the mean of these points as the temperature of that region. Skin and 2-m air temperatures of Montreal are shown in Figure 5 (Control case, CTRL). For the Greater Montreal, the maximum difference between the skin temperature of urban areas and rural areas is about 9 K and it occurred at 1.00 p.m. Thermal storage of the urban surfaces delays the maximum difference of 2-m air temperature to the evenings. As shown in Figure 5, Montreal experienced a 2-m air temperature difference of about 4 K at 8.00 p.m.

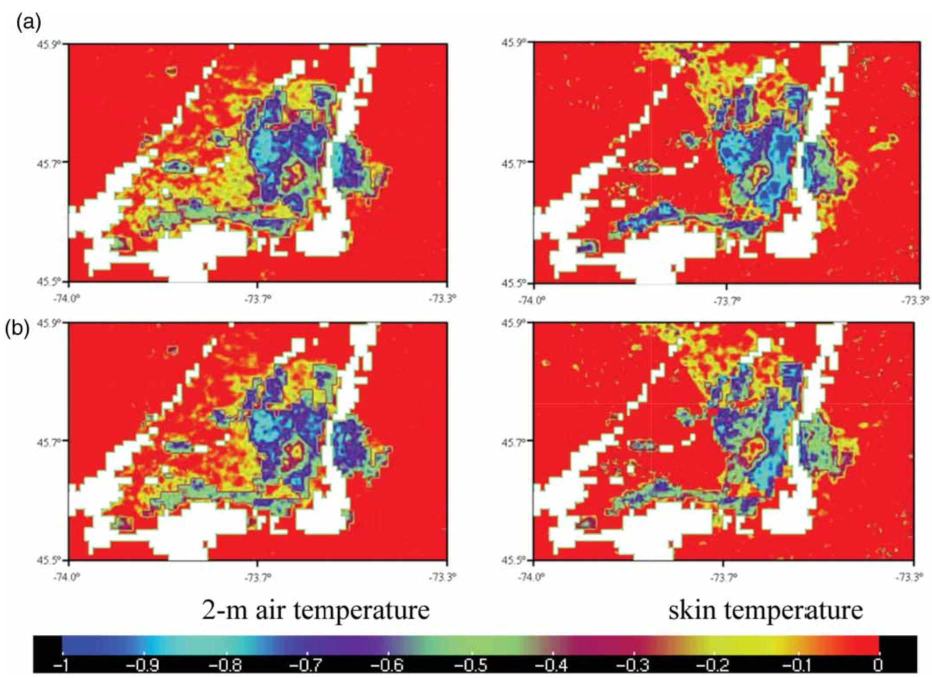

Figure 4. 2-m air temperature and skin temperature difference between (a) ML-UCM and SL-UCM, and (b) ML-UCM and slab model of Greater Montreal in 12 July 2005.

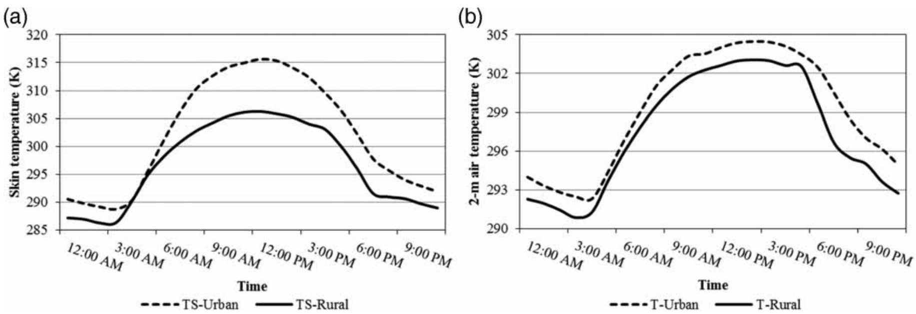

Figure 5. Temporal variation of (a) skin temperature and (b) 2-m air temperature (K) in urban and rural areas of Greater Montreal in 12 July 2005 using ML-UCM for the CTRL case.

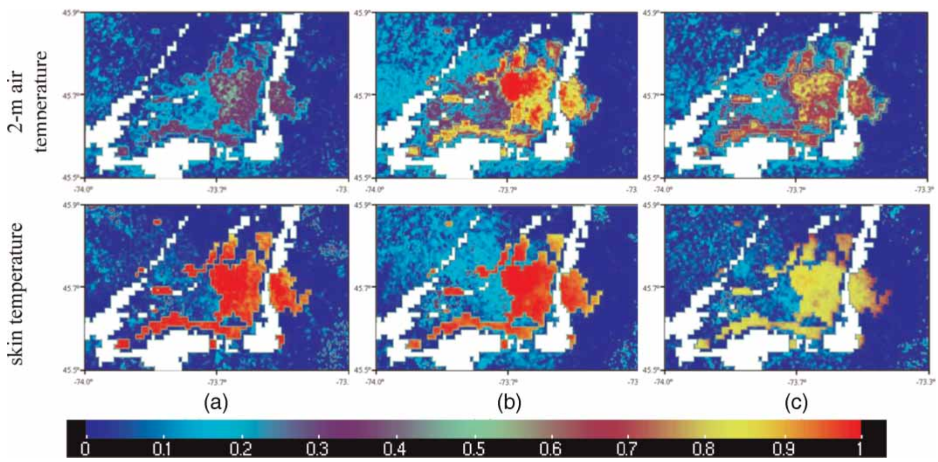

Figure 6. 2-m air temperature and skin temperature difference between CTRL and ALBEDO of Greater Montreal in 12 July 2005. (a) ML-UCM, (b) SL-UCM, and (c) the slab model.

3.3. *Effect of increasing the albedo on urban temperature*

We simulated the effect of increasing the roof albedo (from 0.2 to 0.8) on the air and skin temperatures (Albedo case, ALBEDO). Figure 6 illustrates the results of mean 2-m air and skin temperatures of Greater Montreal. Simulations were performed for all three UCMs to compare their performance in characterizing the modification of the surface. In the slab model, albedo of urban areas increased by 0.2 ($0.35 \times 0.6 \approx 0.2$); roofs considered to cover 35% of the urban area. Increasing albedo of roofs decreased the air temperature of the city about 0.3 K. This value is the change in average temperature; peak temperature reduction is more than that (~1 K)

4. Conclusion

Applicability of using different UCMs for urban climate simulation is investigated. The slab model and SL-UCM overestimated skin and 2-m air temperature by about 1 K compared with ML-UCM. Although the slab model and SL-UCM proved to be effective in large-scale climate simulation, they are not appropriate for urban climate simulations. Consequently, ML-UCM is used to simulate UHI in the city of Montreal. UHI is well observed in urban areas of Montreal.

The maximum difference between urban and rural areas air temperature occurred in the evening. Intensity of UHI was about 4 and 9 K considering 2-m air temperature and skin temperature, respectively. Increasing the albedo of roofs from 0.2 to 0.8 decreased the average air temperature of urban areas of Montreal by 0.3 K. Maximum decrease in air temperature was about 1 K before the noon. Simulations indicated the effectiveness of implementing cool roofs in lowering the summertime temperatures in Montreal.

Acknowledgements

Funding for this research was provided by the National Science and Engineering Research Council of Canada under discovery program.

References

Bornstein, R. D. (1968). Observation of urban heat Island effect in New York city. *Journal of Applied Meteorology*, *7*, 575–583.

Chen, F., & Dudhia, J. (2001). Coupling an advanced land surface–Hydrology model with the Penn State–NCAR MM5 modeling system. Part I: Model implementation and sensitivity. *Monthly Weather Review*, *129*, 569–585.

Chou, M. D., & Suarez, M. J. (1994). *An efficient thermal infrared radiation parameterization for use in general circulation models*. NASA Tech. Memo. 104606, 3, 85pp. Greenbelt, MD: National Aeronautics and Space Administration.

Clough, S., Shephard, M., Mlawer, E., Delamere, J., Iacono, M., Cady-Pereira, K., …Brown, P. D. (2005). Atmospheric radiative transfer modeling: A summary of the AER codes. *Journal of Quantitative Spectroscopy & Radiative Transfer*, *91*, 233–244.

EPA. (2012, August 31). *Heat Island effect*. Retrieved April 9, 2012, from United States Environmental Protection Agency: http://www.epa.gov/hiri/

Grell, G. A., & Devenyi, D. (2002). A generalized approach to parameterizing convection combining ensemble and data assimilation techniques. *Geophysical Research Letters*, *29*(14), Art. no 1693, 38-1–38-4.

Janjic, Z. (1990). The step-mountain coordinate: Physics package. *Monthly Weather Review*, *118*, 1429–1443.

Janjic, Z. (1994). The step-mountain eta coordinate model: Further developements of the convection, viscous sublayer, and turbulence closure schemes. *Monthly Weather Review*, *122*, 927–945.

Janjic, Z. (2002). *Nonsingular implementation of the mellor-yamada level 2.5 scheme in the NCEP meso model*. Camp Springs, MD: National Centers for Environmental Prediction.

Keefer, T. (2012). *AMS glossary*. Retrieved April 9, 2012, from urban heat island: http://amsglossary.allenpress.com/glossary/search?id=urban-heat-island1

Levinson, R., Akbari, H., & Berdahl, P. (2005). Solar spectral optical properties of pigments, part II: Survey of common colorants. *Solar Energy Materials & Solar Cells*, *89*(4), 351–389.

Lin, Y. -L., Farley, R. D., & Orville, H. D. (1983). Bulk parameterization of the snow field in a cloud model. *Journal of Climate and Applied Meteorology*, *22*, 1065–1092.

Liu, Y., Chen, F., Warner, T., & Basara, J. (2006). Verification of a mesoscale data-assimilation and forecasting system for the Oklahoma city area during the joint urban 2003 field project. *Journal of Applied Meteorology and Climatology*, *45*, 912–929.

Mesinger, F., DiMego, G., Kalnay, E., Mitchell, K., Shafran, P. C., Ebisuzaki, W., …Shi, W. (2006). North American regional reanalysis. *Bulletin of Amererican Meteorological Society*, *87*(3), 343–360.

Oke, T. R. (1987). *Boundary layer climates*. New York: Routledge.

Roth, M., Oke, T., & Emery, W. (1989). Satellite-Derived urban heat Islands from three coastal cities and the utilization of such data in urban climatology. *International Journal of Remote Sensing*, *10*, 1699–1720.